A role for eisosomes in maintenance of plasma membrane phosphoinositide levels

Florian Fröhlich[a,b], Romain Christiano[a,b], Daniel K. Olson[a,b], Abel Alcazar-Roman[a,c], Pietro DeCamilli[a,c], and Tobias C. Walther[a,b,d]

[a]Department of Cell Biology and [c]Howard Hughes Medical Institute and Program in Cellular Neuroscience, Neurodegeneration and Repair, Yale School of Medicine, New Haven, CT 06510; [b]Department of Genetics and Complex Diseases, Harvard School of Public Health, Boston, MA 02115; [d]Department of Cell Biology, Harvard Medical School, Boston, MA 02115

ABSTRACT **The plasma membrane delineates the cell and mediates its communication and material exchange with the environment. Many processes of the plasma membrane occur through interactions of proteins with phosphatidylinositol(4,5)-bisphosphate ($PI(4,5)P_2$), which is highly enriched in this membrane and is a key determinant of its identity. Eisosomes function in lateral organization of the plasma membrane, but the molecular function of their major protein subunits, the BAR domain–containing proteins Pil1 and Lsp1, is poorly understood. Here we show that eisosomes interact with the $PI(4,5)P_2$ phosphatase Inp51/Sjl1, thereby recruiting it to the plasma membrane. Pil1 is essential for plasma membrane localization and function of Inp51 but not for the homologous phosphatidylinositol bisphosphate phosphatases Inp52/Sjl2 and Inp53/Sjl3. Consistent with this, absence of Pil1 increases total and available $PI(4,5)P_2$ levels at the plasma membrane. On the basis of these findings, we propose a model in which the eisosomes function in maintaining $PI(4,5)P_2$ levels by Inp51/Sjl1 recruitment.**

Monitoring Editor
David G. Drubin
University of California, Berkeley

Received: Nov 5, 2013
Revised: Jul 7, 2014
Accepted: Jul 15, 2014

INTRODUCTION

The plasma membrane forms the boundary of cells. It mediates all communication and transport in and out of cells. To perform the many cellular processes mediating these functions, the composition of the plasma membrane is distinct from that of other cellular membranes and is regulated during changing conditions. For example, sphingolipids and sterols are predominantly present in the outer leaflet of the plasma membrane, where they are believed to provide a tight membrane seal. In the cytoplasmic leaflet of the plasma membrane, phosphatidylinositol(4,5)-bisphosphate ($PI(4,5)P_2$) is highly enriched compared with other cellular membranes and interacts with a set of plasma membrane–specific proteins. These interactions provide spatial specificity for many biochemical reactions that occur at the plasma membrane, such as endocytosis, exocytosis, and cell signaling.

$PI(4,5)P_2$ is generated at the plasma membrane by phosphorylation of phosphatidylinositol. The kinase reactions are counteracted by phosphoinositide phosphatases. Mechanisms that control the localization of these enzymes play a major role in achieving $PI(4,5)P_2$ homeostasis. Mammalian cells express nine $PI(4,5)P_2$ phosphatases, which have different tissue distributions (Pirruccello and De Camilli, 2012). Whereas numerous studies have addressed specific functions of these enzymes, elucidation of basic principles, such as their shared and/or specific functions, have been complicated by their large number. The genome of the yeast *Saccharomyces cerevisiae* encodes only three such enzymes—Inp51/Sjl1, Inp52/Sjl2, and Inp53/Sjl3 (Srinivasan *et al.*, 1997; Singer-Kruger *et al.*, 1998; Stolz *et al.*, 1998)—whose roles in maintaining appropriate $PI(4,5)P_2$ levels remain largely unknown. Analysis of one such isoform, Inp52, revealed an important function specifically during actin patch–mediated endocytosis (Singer-Kruger *et al.*, 1998; Stefan *et al.*, 2005; Sun *et al.*, 2007), suggesting that phosphatases might play specialized roles in different plasma membrane processes. It is expected that

This article was published online ahead of print in MBoC in Press (http://www.molbiolcell.org/cgi/doi/10.1091/mbc.E13-11-0639) on July 23, 2014.

Address correspondence to: Tobias Walther (twalther@hsph.harvard.edu), Florian Fröhlich (froehlic@hsph.harvard.edu).

Abbreviations used: BAR domain, Bin1, amphiphysin, Rvs161/167 domain; CC, correlation coefficient; E-MAP, epistatic mini array profile; GFP, green fluorescent protein; MCC, membrane compartment containing Can1; MS, mass spectroscopy; PH domain, pleckstrin homology domain; PI(3)P, phosphatidylinositol 3-phosphate; PI(4)P, phosphatidylinositol 4-phosphate; $PI(4,5)P_2$, phosphatidylinositol(4,5)-bisphosphate; SILAC, stable isotope labeling with amino acids in cell culture.

further analysis of the function of these enzymes in yeast may help to shed light on fundamental PI(4,5)P_2 metabolism.

The plasma membrane is not only distinct in its composition from other membranes, but it is also organized into lateral compartments of distinct protein and lipid composition. In the yeast *Saccharomyces cerevisiae,* the plasma membrane contains a number of domains that appear either as punctate foci or networks of percolating proteins (Malinska *et al.*, 2003, 2004; Berchtold and Walther, 2009; Ziolkowska *et al.*, 2012). Staining with lipid-binding dyes, such as filipin, further suggests that lipids, such as ergosterol, are unevenly distributed between the domains (Grossmann *et al.*, 2007).

One prominent plasma membrane domain is the membrane compartment containing Can1 (MCC), which ultrastructurally is defined by distributed membrane furrows directed toward the cytoplasm (Stradalova *et al.*, 2009; Karotki *et al.*, 2011; Moreira *et al.*, 2012). MCC domains are formed by large protein complexes peripherally associated with the furrows, termed eisosomes (Walther *et al.*, 2006; Karotki *et al.*, 2011). Eisosomes consist primarily of two homologous, highly abundant core subunits, Pil1 and Lsp1, both present at an abundance of ~100,000 copies/cell, as well as a host of substoichiometric proteins of mostly unclear function (Aguilar *et al.*, 2010; Moreira *et al.*, 2012). Pil1 and Lsp1 contain Bin1, amphiphysin, Rvs161/167 (BAR) domains (Olivera-Couto *et al.*, 2011; Ziolkowska *et al.*, 2011) and assemble into helical half-cylinders at the plasma membrane, molding the membrane into an ~50-nm-deep, ~200- to 300-nm-long furrow (Stradalova *et al.*, 2009; Karotki *et al.*, 2011). Among eisosome proteins, Pil1 is particularly important for the architecture of the complex. In its absence, the normally distributed eisosome pattern collapses, and MCC and eisosome proteins localize to one or a few remnants that represent large, aberrant plasma membrane invaginations (Walther *et al.*, 2006; Stradalova *et al.*, 2009).

Membrane interactions of Pil1 and Lsp1 are likely mediated by a short N-terminal protein segment and a patch of positively charged amino acids in their BAR domains, which specifically interact with negatively charged lipid head groups, for example, of PI(4,5)P_2. Consequently, gross alterations of PI(4,5)P_2 levels—for example, due to inactivation of the only yeast plasma membrane phosphatidylinositol 4-phosphate (PI(4)P) kinase, Mss4—reduce plasma membrane association of Pil1 and Lsp1 (Karotki *et al.*, 2011).

Membrane organization by eisosomes is important for control of cell signaling. Studies of sphingolipid signaling revealed that the organization of the plasma membrane into eisosomes and domains containing the target of rapamycin complex 2 (TORC2) kinase is crucial for detection of membrane stress and alteration of sphingolipid levels (Berchtold and Walther, 2009; Berchtold *et al.*, 2012; Frohlich *et al.*, 2009).

Here we analyze genetic interactions of eisosome core components to reveal a specific connection of Pil1 with the PI(4,5)P_2 phosphatase Inp51, also known as synaptojanin-like protein 1 (Sjl1). We find that Pil1 specifically recruits Inp51 to the plasma membrane and is crucial for maintaining normal plasma membrane phosphatidylinositide levels and availability.

RESULTS

The phosphatidylinositol bisphosphate phosphatases Inp51, Inp52, and Inp53 have distinct cellular functions

To investigate the physiological function of *PIL1* in membrane organization, we analyzed its genetic interactions, systematically measured in an epistatic mini array profile (E-MAP; Schuldiner *et al.*, 2005, 2006; Collins *et al.*, 2006; Breslow *et al.*, 2008; Aguilar *et al.*, 2010; Hoppins *et al.*, 2011). Specifically, we used an E-MAP data set containing ~700 genes involved in lipid metabolism and membrane trafficking, as well as the gene encoding the eisosome component Pil1 (Surma *et al.*, 2013).

First, we analyzed correlations of genetic interaction profiles in the E-MAP. If two mutations have similar physiological functions, they likely share suppressing and aggravating genetic interactions with other mutations, resulting in highly similar genetic interaction profiles. We find that *PIL1* and *INP51* have the highest correlation with each other in the lipid E-MAP (Figure 1, a and b; correlation coefficient [CC] = 0.54), suggesting that these genes function together or in similar processes. In contrast, we did not find significant correlations between *PIL1* and the other two PI(4,5)P_2 phosphatase genes, *INP52* and *INP53* (Figure 1, c and d; CC = 0.10 and 0.06, respectively). Similar correlations between *PIL1* and *INP51* are present in another E-MAP focusing on genes implicated in plasma membrane function (F.F. and T.C.W., unpublished data; Aguilar *et al.*, 2010; Karotki *et al.*, 2011).

INP52 has the highest correlations with genes encoding endocytic actin patch proteins, such as *ABP1* or *SLA1* (Figure 1, a and c; CC = 0.39 and 0.34). Consistent with previous results characterizing Inp52 function, these data highlight its function in actin-dependent endocytosis (Singer-Kruger *et al.*, 1998; Stefan *et al.*, 2005; Sun *et al.*, 2007). Genetic interactions of *INP53* correlate well with the profiles *of VPS30* and *VPS38*, both encoding subunits of phosphatidylinositol 3-kinase. This complex is involved in endosomal and autophagy trafficking (Figure 1, a and d; *VPS30* CC = 0.59 and *VPS38* CC = 0.58), suggesting Inp53 functions in these processes. The correlations of Inp51, Inp52, and Inp53 phosphoinositide phosphatases with actin patches, eisosomes, or endosomal trafficking are specific, as there is little cross-correlation between each particular phosphoinositide phosphatase (Figure 1e) and the processes related to any of their homologues (Figure 1, b–d).

Inp51 localizes to eisosomes

Genetic interactions suggest that Inp51, Inp52, and Inp53 phosphoinositide phosphatases function in different processes, predicting potentially different subcellular localizations. To test this hypothesis directly for phosphoinositide phosphatase function at the plasma membrane, we investigated the localization of Inp51, Inp52, and Inp53 with respect to eisosomes and actin patches. We inserted the sequence encoding the green fluorescent protein (GFP) fluorophore at the 3′ end of the open reading frame of *INP51, INP52*, or *INP53* at their respective genomic loci, driving their expression from their endogenous promoters. Analysis by confocal fluorescence microscopy shows that Inp51 localizes in a punctate pattern at the plasma membrane. Inp51 spots colocalize with eisosomes, marked with red fluorescently tagged Lsp1 (Figure 2a, left; quantification in Figure 3c) but was excluded from actin patches marked with Abp1 fused to red fluorescent protein (Figure 2a, right). Localization of Inp51 at static eisosomes is highly dynamic (Figure 3a and Supplemental Movie S1). The residence time of an Inp51 focus at a particular eisosome varied greatly, ranging from <2 to >30 s (Figure 3b).

Similarly, Inp52 localized in a punctate pattern at the plasma membrane. However, we did not observe colocalization with eisosomes (Figure 2b, left) but instead with a subset of endocytic actin patches (Figure 2b, right), as observed previously (Stefan *et al.*, 2005; Sun *et al.*, 2007).

Compared with Inp51 and Inp52 localization, Inp53 showed a distinct pattern with little or no signal at the plasma membrane and did not colocalize with either Lsp1 or Abp1 (Figure 2c, left and right). Instead, it formed larger foci within the cytoplasm (Figure 2c, right). Because the genetic interaction analyses suggest a function of Inp53 in endosomal trafficking, this signal might correspond to endosomes.

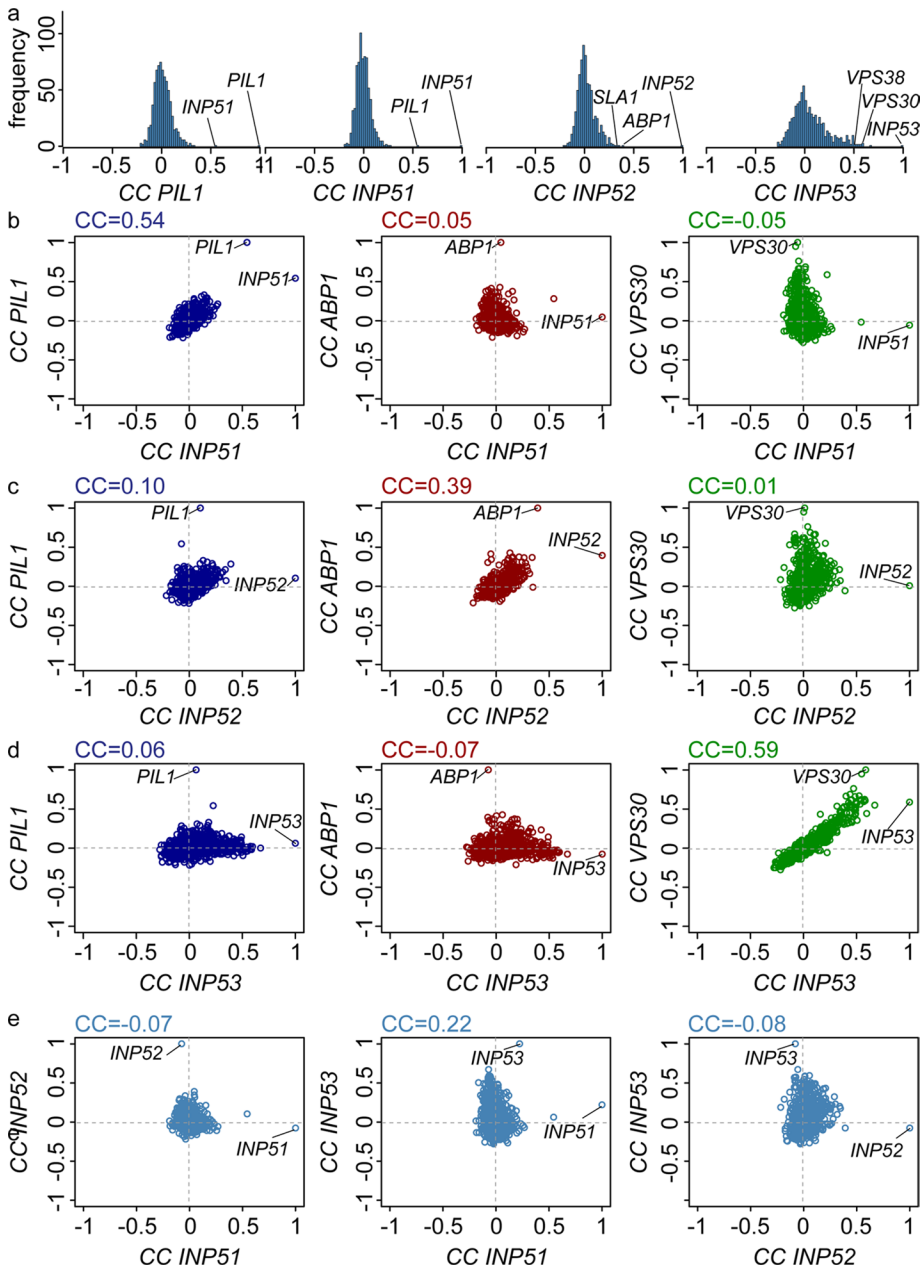

FIGURE 1: Global analysis of all phosphoinositide phosphatase and *PIL1* genetic interactions. (a) Histograms of correlation coefficients generated by comparing the profiles of genetic interactions for each phosphoinositide phosphatase and Pil1 to all other profiles in the E-MAP analysis. *PIL1* and *INP51* display the strongest correlation to each other. *INP52* shows correlation with genes encoding actin patch proteins. *INP53* is correlated with genes encoding the endosomal phosphatidylinositol 3,5-bisphosphate kinase. (b) Genes with correlating genetic profiles are shared between *INP51* and *PIL1* but not *INP51* and *ABP1* or *VPS30*. Correlation coefficients between the genetic profile of *INP51* and each of the other profiles in the E-MAP are plotted on the *x*-axis. Plotted on the *y*-axis are the similar sets of values for the *PIL1* profile with all other profiles (blue), those for *ABP1* with all other profiles (red), or those for *VPS30* with all other profiles (green). CC values in blue, red, and green indicate the correlation coefficients for the full set of blue, red, and green points plotted. (c) Genes with correlating genetic profiles are shared between *INP52* and *ABP1* but not *INP52* and *PIL1* or *VPS30*. (d) Genes with correlating genetic profiles are shared between *INP53* and *VPS30* but not *INP52* and *PIL1* or *ABP1*. (e) *INP51*, *INP52*, and *INP53* do not correlate with each other.

Inp51 physically interacts with eisosomes

Our data reveal specialized functions for phosphoinositide phosphatases, as well as spatial segregation of Inp51 and Inp52 at the plasma membrane. Localization of Inp51 to eisosomes and its genetic correlation and suppression of genetic interaction with *Pil1* (Figures 1 and 2 and Supplemental Figure S1) suggest that eisosomes may physically interact with Inp51. To test this hypothesis, we immunopurified GFP-tagged Inp51 from cells metabolically labeled with "heavy," nonradioactive lysine 8 (stable isotope labeling with amino acids in cell culture [SILAC]; Ong *et al.*, 2002). In parallel, we performed a mock purification from wild-type (WT) cells labeled with normal ("light") lysine. We mixed eluates from both purifications and analyzed them by high-resolution mass spectrometry–based proteomics (Walther and Mann, 2010). Peptides from proteins containing the "heavy" isotope–labeled lysine are shifted right in the spectra compared with the same peptide from unlabeled protein, allowing quantitation of abundance ratios for each detected peptide and protein from the eluates.

In these experiments, we identified Inp51 as the most enriched protein in eluates from strains expressing the GFP-tagged form compared with controls. We also detected the known regulator Irs4 as a specific interactor of Inp51 (Morales-Johansson *et al.*, 2004). In addition, we identified several known eisosome proteins, including the eisosome core proteins Pil1 and Lsp1, as well as Eis1, Seg1, Msc3, and Ygr130C as highly specific interactors of Inp51 (Figure 4a; Aguilar *et al.*, 2010; Moreira *et al.*, 2012).

To assay independently for the interaction of Inp51 and eisosomes, we also purified GFP-tagged Pil1 from "heavy"-labeled yeast cells and compared it with a mock purification from "light"-labeled WT cells. We identified all known eisosome interacting proteins—Lsp1, Eis1, Seg1, Ygr130C, Msc3, Pkh1, and Ykl105C. In addition, we identified Inp51 as a significantly enriched protein (Figure 4b).

The specificity of the interaction between Inp51 and eisosomes is particularly apparent when the experiments are compared with one another. We plotted the heavy/light ratios of proteins from the Inp51 pull down versus the ratios of proteins from the Pil1 pull downs. As expected, the majority of proteins detected are contaminants not enriched in both experiments. The specific interactors from both pull downs localize to the top right quadrant of the plot and show all known eisosome components (Pil1, Lsp1, Seg1, Ykl105c, Eis1, Ygr130C, and Msc3), as well as Inp51 and its known regulator, Irs4 (Figure 4c). We did not find evidence for the interaction of

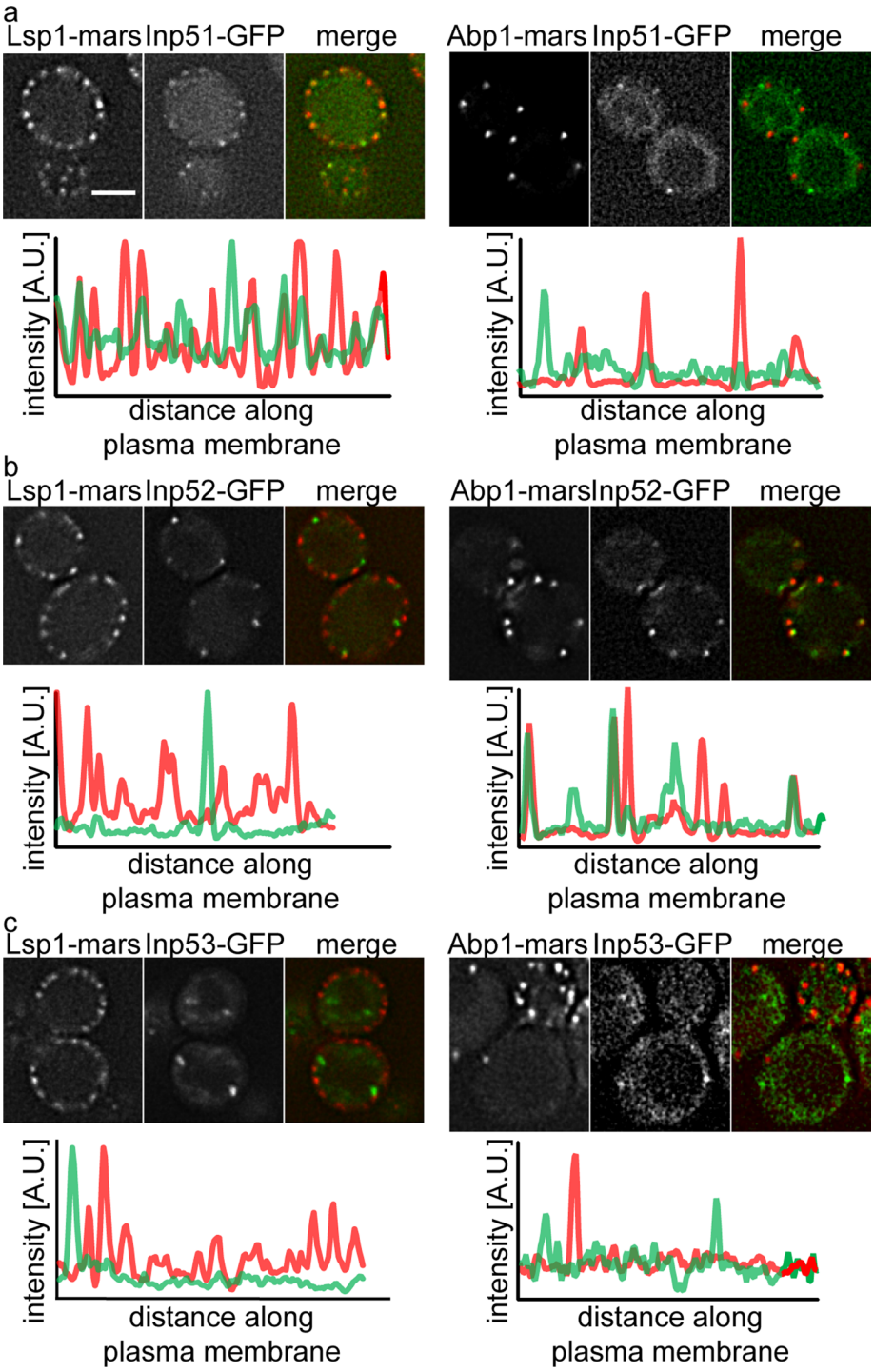

FIGURE 2: The three yeast phosphatidylinositol bisphosphate phosphatases localize to different compartments within cells. (a) Colocalization of GFP-tagged Inp51 with RFPmars-tagged Lsp1 (left) and RFPmars-tagged Abp1 (right). Representative confocal midsections. The graphs show the intensity profiles for both channels along the perimeter of the cell. (b) Colocalization of GFP-tagged Inp52 with RFPmars-tagged Lsp1 (left) and RFP-mars-tagged Abp1 (right). Representative confocal midsections. The graphs show the intensity profiles for both channels along the perimeter of the cell. (c) Colocalization of GFP-tagged Inp53 with RFPmars-tagged Lsp1 (left) and RFP-mars-tagged Abp1 (right). Representative confocal midsections. The graphs show the intensity profiles for both channels along the perimeter of the cell. Scale bar, 2.5 μm.

eisosome components with Inp52 or Inp53, suggesting that the interaction of eisosomes with Inp51 is specific for this phosphoinositide phosphatase.

Inp51 localization to the plasma membrane is Pil1 dependent

Motivated by the genetic, cell biological, and biochemical data, we next tested whether eisosomes recruit Inp51 to the plasma membrane. We analyzed Inp51 localization in *pil1Δ* cells by fluorescence microscopy. We did not observe Inp51 at the plasma membrane in a *pil1Δ* strain, compared with many foci in WT cells (Figure 5a, Supplemental Figure S2, and Supplemental Movie S2). To test whether Inp51 is mislocalized or degraded in *pil1Δ* cells, we analyzed Inp51-GFP levels in WT and *pil1Δ* cells after immunoprecipitation. We did not observe any differences in protein levels, suggesting that Inp51 is not degraded but fails to target the plasma membrane in the absence of Pil1 (Supplemental Figure S2b). Of importance, the effect of *PIL1* deletion was specific to Inp51 localization, as we did not observe any significant changes in Inp52 and Inp53 localization in this strain (Figure 5, b and c). Eisosome-dependent recruitment of Inp51 to the plasma membrane required specifically Pil1, as deletion of the highly homologous Lsp1 subunit did not have an effect on Inp51 localization (Supplemental Figure S3).

To further test whether deletion of *PIL1* interferes with Inp51 function at the plasma membrane, we tested for genetic interactions of *pil1Δ* with *inp52Δinp53Δ*. Synaptojanin triple-knockout mutations are lethal (Stolz *et al.*, 1998; Figure 6a). As expected if Inp51 function is dependent on recruitment to the plasma membrane by Pil1, deletion of *PIL1* in an *inp52Δinp53Δ* strain yielded a strong synthetic growth defect phenocopying the effects of a synaptojanin triple mutant (Figure 6b).

Capitalizing on this genetic assay, we tested whether other known eisosome components are required for normal Inp51 function. We did not detect genetic interactions between any of the known eisosome components, *LSP1*, *EIS1*, *YGR130C*, *SEG1*, *YKL105C*, or *MSC3*, and *inp52Δinp53Δ*. Thus specifically Pil1 is required for Inp51 function (Figure 6c and Supplemental Figure S4).

The genetic interaction with *inp52Δinp53Δ* allowed us to test requirements of specific Pil1 features, such as the C-terminal extension from the BAR domain (Ziolkowska *et al.*, 2011) or phosphorylation sites, for Inp51 function. In summary, these experiments showed that the BAR domain of Pil1 is sufficient to rescue synthetic lethality when combined with *inp52Δinp53Δ* mutants and that phosphorylation at the Pkc1-dependent phosphorylation sites (S230 and T233; Mascaraque *et al.*, 2013) is not required (Supplemental Figure S5).

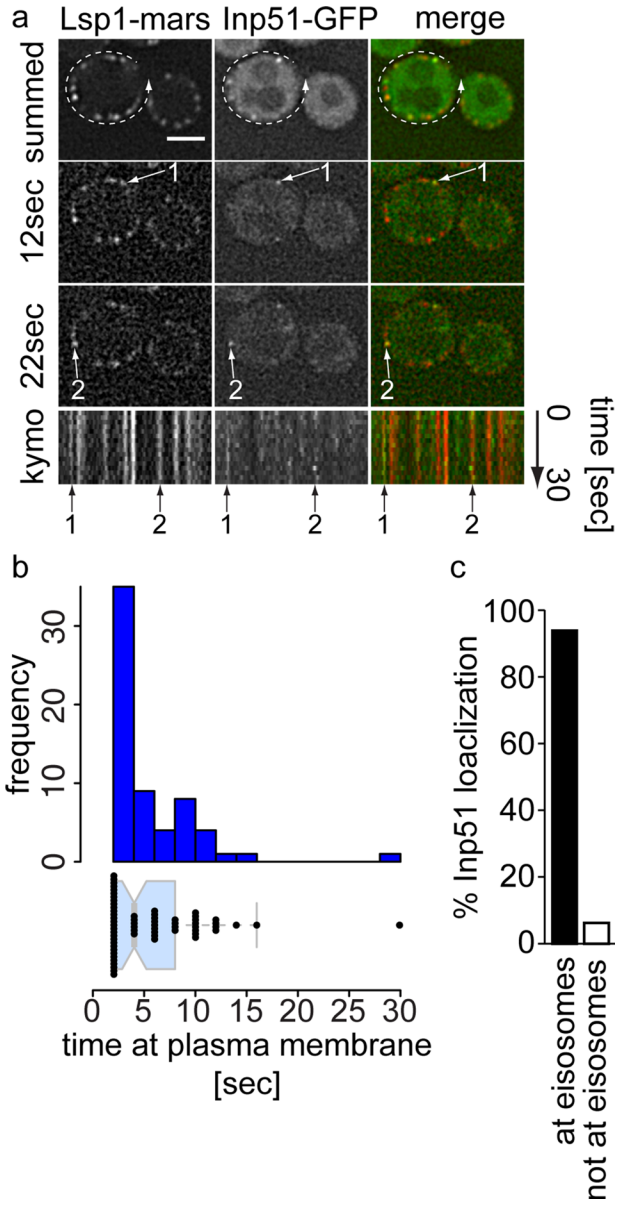

FIGURE 3: Inp51 localization at the plasma membrane is dynamic. (a) The Inp51 pattern at the plasma membrane changes rapidly. Images of cells expressing Inp51-GFP and Lsp1-RFPmars were collected in 2-s intervals for 30 s. Top, summed intensities of the whole time course for Lsp1-RFPmars (left), Inp51-GFP (middle), and the merged channels (right). Bottom, white dotted arrow indicates start and end points for the kymographs. Middle, representative images of the time course at 12 and 22 s. Arrows highlight specific foci in the images and the kymographs. (b) Quantification of Inp51-GFP residence time at the plasma membrane. The histogram shows the residence time of Inp51 foci ($n = 63$). Average residence time of the foci is 4 s as shown in the density dot plot. Scale bar, 2.5 μm. (c) Quantification of Inp51-GFP spots colocalizing with eisosomes as percentage of total.

Pil1 controls phosphatidylinositol bisphosphate plasma membrane levels by recruitment of Inp51

It is unknown how plasma membrane phosphoinositide levels are regulated in yeast. Recruitment of Inp51 to eisosomes suggests that these plasma membrane domains may have an important function in lipid homeostasis. To test this hypothesis, we assayed phosphoinositide levels in *pil1Δ*, *inp51Δ*, and *pil1Δinp51Δ* double-mutant cells compared with WT cells. We found that total cellular levels of phosphatidylinositol 3-phosphate (PI(3)P) were not significantly changed in mutants compared with WT cells. As expected, there was a robust increase in PI(4,5)P_2 levels (1.6 times) with a concomitant decrease in PI(4)P levels in *inp51Δ* cells (Figure 7a). We also observed a statistically significant increase in PI(4,5)P_2 levels in cells lacking *PIL1* (1.3 times). Of interest, PI(4,5)P_2 levels of a *pil1Δinp51Δ* double knockout were the same as in a *pil1Δ* single-mutant strain.

To determine PI(4,5)P_2 localization in the different mutant strains, we integrated a construct containing two pleckstrin homology (PH) domains of mammalian phospholipase Cδ (PLCδ) fused to GFP under the control of the CPY promoter (GFP-2xPH_{PLC}) into the genome of WT, *pil1Δ*, *inp51Δ*, or *pil1Δinp51Δ* cells and measured GFP fluorescence intensity at the plasma membrane and in the cytoplasm. We found a small but statistically significant ($p < 0.01$) 20% increase of GFP signal from our PI(4,5)P_2 reporter construct at the plasma membrane in *inp51Δ* cells compared with WT cells.

Surprisingly, we observed an even larger signal increase at the plasma membrane of *pil1Δ*, as well as *pil1Δinp51Δ* cells (1.9- and 1.5-fold, respectively; Figure 7b; quantitation in Figure 7, c and d). We obtained similar results when expressing the PH domain of Slm1, whose localization in our hands is highly sensitive to plasma membrane PI(4,5)P_2 levels in *pil1Δ* cells (Supplemental Figure S6). These data suggest that free PI(4,5)P_2 amounts available for protein binding are increased even more than the total cell levels of this lipid. Total protein levels of the GFP-2xPH_{PLC} reporter construct were elevated in *pil1Δ* and *pil1Δinp51Δ* cells, likely indicating that PI(4,5)P_2-bound reporter is protected from turnover (Figure 7, e and f).

DISCUSSION

We systematically analyzed the role of the different yeast phosphoinositide phosphatases. Our data and previous reports taken together suggest that Inp53 functions at endosomes. Of the two plasma membrane–localized phosphoinositide phosphatases, Inp52 is a component of endocytic actin patches, with a distinct time point during the biogenesis of the patch when it is recruited and leaves, suggesting it is part of the core machinery executing clathrin-mediated endocytosis (Singer-Kruger *et al.*, 1998; Stefan *et al.*, 2005; Sun *et al.*, 2007). This function is very similar to the one proposed for synaptojanin in clathrin-mediated endocytosis in mammalian cells (Cremona *et al.*, 1999; Di Paolo and De Camilli, 2006).

In contrast, Inp51 is excluded from actin patches and localizes in a highly dynamic manner to eisosomes instead. Pil1 is required for Inp51 recruitment to eisosomes, and the proteins physically interact with each other. We observe Inp51 localization as clearly distinct from actin patches and do not observe Inp52 or Inp53 on eisosomes. In addition, the different genetic interaction profiles of Inp51 and Inp52 support the notion of different functions of the two phosphatases. Therefore our data indicate a specific function for Pil1 with Inp51 rather than a suggested more general role of Pil1 in recruiting several phosphoinositide phosphatases (Murphy *et al.*, 2011).

Thus Pil1 and Inp51 functioning together presents another instance of a specific BAR domain protein and a synaptojanin-like phosphatase acting together. This is similar to the cooperation of Rvs161/Rvs167 with Inp52 in endocytic actin patches and endophilin with synaptojanin in metazoan cells (Milosevic *et al.*, 2011). This likely highlights the generality and ancient origin of this function of BAR domain–containing proteins.

How eisosomes recruit Inp51 mechanistically remains unknown. Our analyses of synthetic phenotypes of eisosome components with

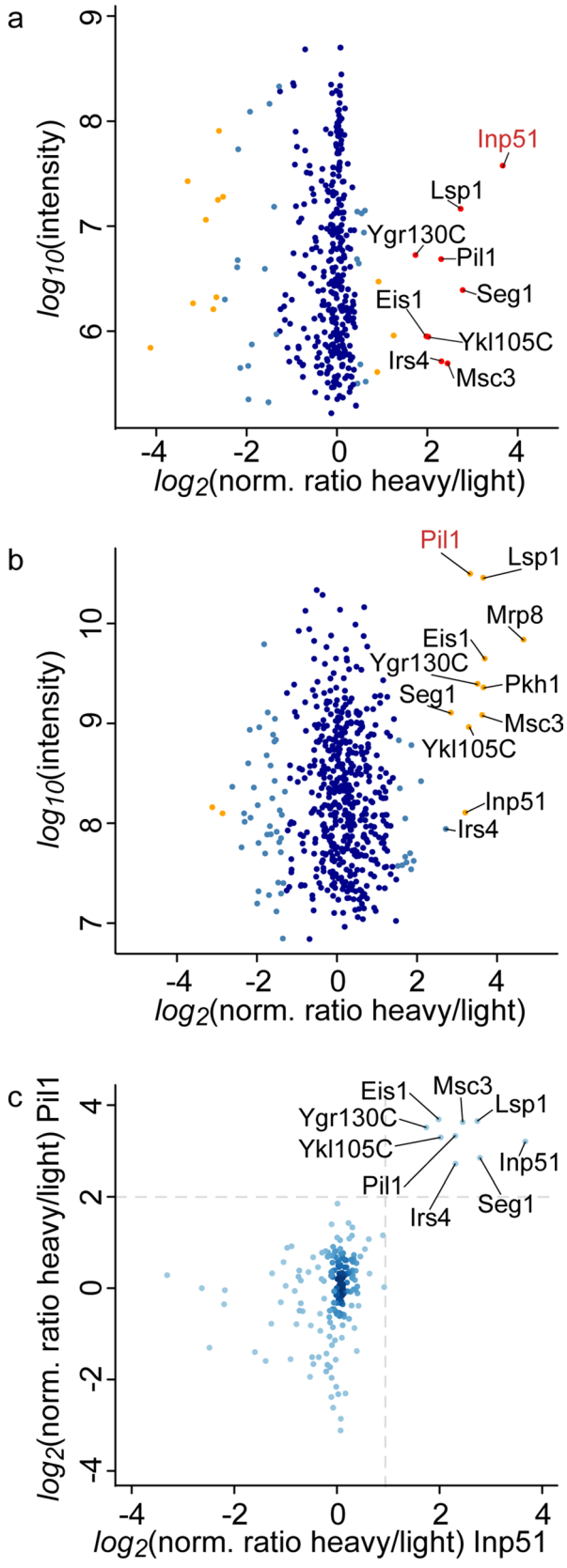

FIGURE 4: Inp51 physically interacts with Pil1. (a) Affinity purification and MS analysis of "heavy"-labeled cells expressing GFP-tagged Inp51 and untagged control cells. Intensities are plotted against normalized heavy/light SILAC ratios. Significant outliers ($p < 1e\text{-}11$) are colored in red, orange ($p < 0.0001$), or light blue ($p < 0.05$); other identified proteins are shown in dark blue. (b) Affinity purification and MS analysis of "heavy"-labeled cells expressing GFP-tagged Pil1 and untagged, "light"-labeled control cells. Intensities are plotted against normalized heavy/light SILAC ratios. Significant outliers ($p < 1e\text{-}11$) are colored in red, orange ($p < 0.0001$), or light blue ($p < 0.05$); other identified proteins are shown in dark blue. (c) Proteins identified in both the Inp51-GFP and Pil1-GFP pull downs are plotted against each other. Color coding is according to density, with darker colors showing an enrichment of spots. Outliers that are significant in both pull downs are labeled.

inp52Δinp53Δ show that specifically Pil1, but none of the other known eisosome components, is required to maintain Inp51 function. Consistent with this model, Inp51 does not localize to eisosome remnants containing the remaining components of the complex in *pil1Δ* cells. We thus posit that Pil1 might directly contact Inp51 or a protein with which it is in complex, such as Irs4. Pil1 assembles into a semicylindrical protein coat with Lsp1 in eisosomes. Crystallographic and electron tomographic data (Karotki *et al.*, 2011; Ziolkowska *et al.*, 2011) show that the flexible C-terminal tail of Pil1 points from this structure toward the cytoplasm. However, our genetic interactions show that this Pil1 tail is not required for Inp51 function at the plasma membrane. Instead, a Pil1-fourth helix of the Pil1 BAR domain not found in other domains of this family was required for the interaction. However, in the absence of this helix, eisosomes fail to assemble normally, complicating the interpretation of this mutation (unpublished data).

Pil1 and Lsp1 are heavily phosphorylated. In Pil1 there are at least 11 phosphorylation sites that are targets of the Pkh1/2 and Pkc1 pathways, which mediate signaling in response to lipid and plasma membrane changes (Luo *et al.*, 2008; Frohlich *et al.*, 2009; Mascaraque *et al.*, 2013). Some of these phosphorylation sites regulate Pil1 and Lsp1 assembly (Walther *et al.*, 2007; Luo *et al.*, 2008). Another phosphorylation site (S59) lies within a pocket of the Pil1 and Lsp1 BAR domains facing the plasma membrane and is required for $PI(4,5)P_2$ binding (Ziolkowska *et al.*, 2011). Still other phosphorylation sites are found on the BAR domain or in the C-terminal region outside of the BAR domain. We ruled out in genetic experiments for some of these sites that they are important for Inp51 recruitment (S230 and T233). Other sites might regulate Inp51 recruitment, which might help coordinate the need for $PI(4,5)P_2$ at the plasma membrane.

We find that the total cellular amount of $PI(4,5)P_2$, as well as the amount available for protein binding, is increased in *pil1Δ* mutants. Because endocytosis and actin are regulated by plasma membrane $PI(4,5)P_2$, this increase may explain at least some of the phenotypes observed on actin patches and the endocytic efficiencies for a variety of cargoes in *pil1Δ* cells (Walther *et al.*, 2006; Grossmann *et al.*, 2008; Brach *et al.*, 2011; Murphy *et al.*, 2011).

What is the function of eisosomes and their recruitment of Inp51/Slj1 in phosphoinositide metabolism? Our working model is that Pil1 and Inp51 function to maintain adequate levels of $PI(4,5)P_2$ at the plasma membrane. Pil1 (and Lsp1) BAR domains each contain a binding site for $PI(4,5)P_2$. Their assembly in an eisosome, which contains hundreds of each of the proteins, thus likely recruits and clusters these lipids in the plasma membrane. Consistent with this notion, we observe that the absence of Pil1 leads to increased $PI(4,5)P_2$ available for binding and a more modest increase of total levels. In contrast, deletion of *INP51* results in a larger amount of total $PI(4,5)P_2$ levels, with a mild increase in the $PI(4,5)P_2$ levels available for binding. The hundreds of binding sites on Pil1 and Lsp1 might thus normally bind a large pool of available $PI(4,5)P_2$ to buffer for fluctuations in availability of this lipid by binding or releasing it at

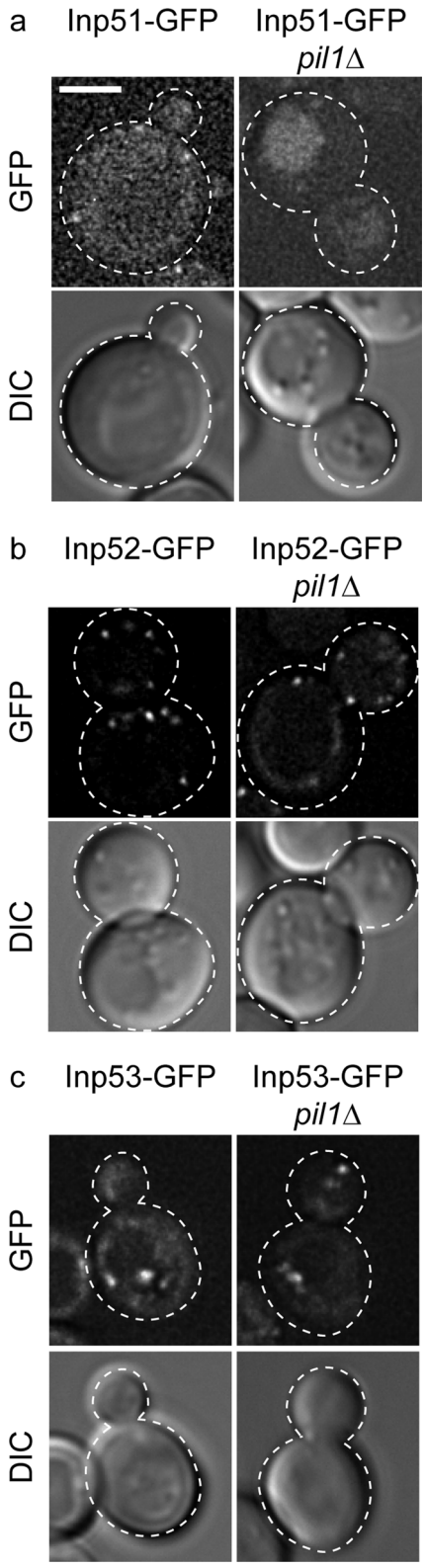

FIGURE 5: *PIL1* is required for normal localization of Inp51. (a) Inp51-GFP was expressed and imaged either in WT or *pil1Δ* cells. Representative confocal midsections. Pil1 is not required for regular distribution of Inp52 (b) or Inp53 (c). Scale bar, 2.5 μm.

concentrations around the K_d of the interaction. In the absence of Pil1, this PI(4,5)P_2 is free in the plasma membrane and can be bound by the reporter. It is possible that this free pool of PI(4,5)P_2 becomes

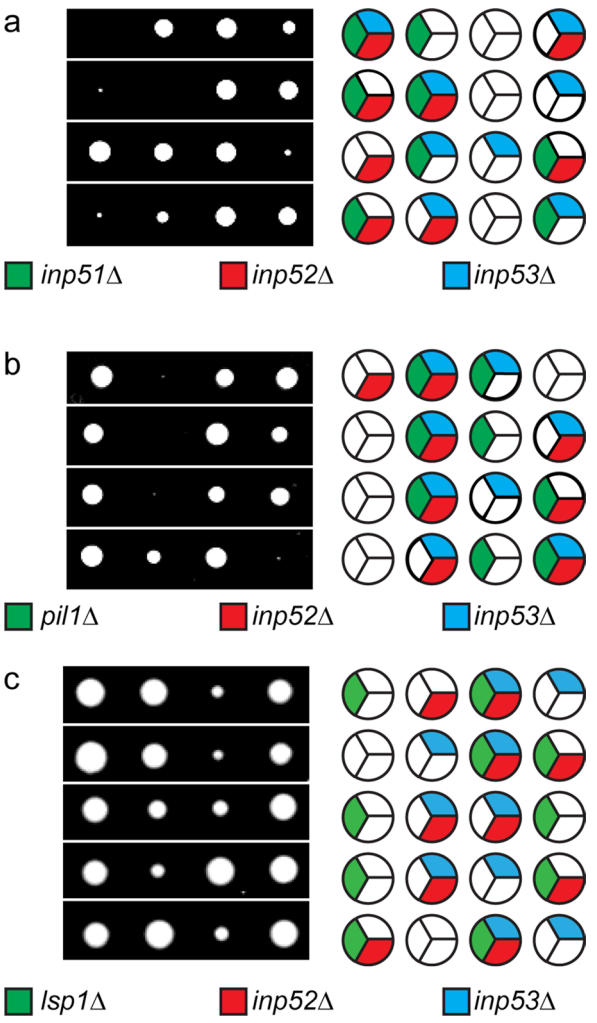

FIGURE 6: *PIL1* genetically interacts with *INP52* and *INP53*. (a) Tetrad analysis of *inp51Δ* mutants crossed with *inp52Δinp53Δ*. (b) Tetrad analysis of *pil1Δ* mutants crossed with *inp52Δinp53Δ*. (c) Tetrad analysis of *lsp1Δ* mutants crossed with *inp52Δinp53Δ*.

available as a substrate for Inp52 or Inp53. The sequestering of PI(4,5)P_2 by Pil1 binding might operate in concert with recruitment of Inp51 to eisosomes to regulate PI(4,5)P_2 availability and turnover. In our model, these mechanisms together maintain normal plasma membrane phosphoinositide levels.

MATERIALS AND METHODS

Strains and plasmids

All yeast strains used in this study and their genotypes are listed in Supplemental Table S1, as are all plasmids used in this study. Standard yeast manipulations, including transformation, homologous recombination of PCR-generated fragments, and tetrad dissections, were performed as described previously (Janke *et al.*, 2004; Berchtold and Walther, 2009; Frohlich *et al.*, 2009).

The $CPY_{promotor}$-2x$GFP_{PLC\delta}$ plasmid was created by cloning this construct from pRS426GFP-2×$PH_{PLC\delta}$ (Stefan *et al.*, 2002) into the *Not*I and *Hind*III sites of pRS306.

Yeast culture

All experiments were performed on yeast grown at 30°C. For microscopy, cells were grown in synthetic complete medium and bound to concanavalin A–treated coverslips.

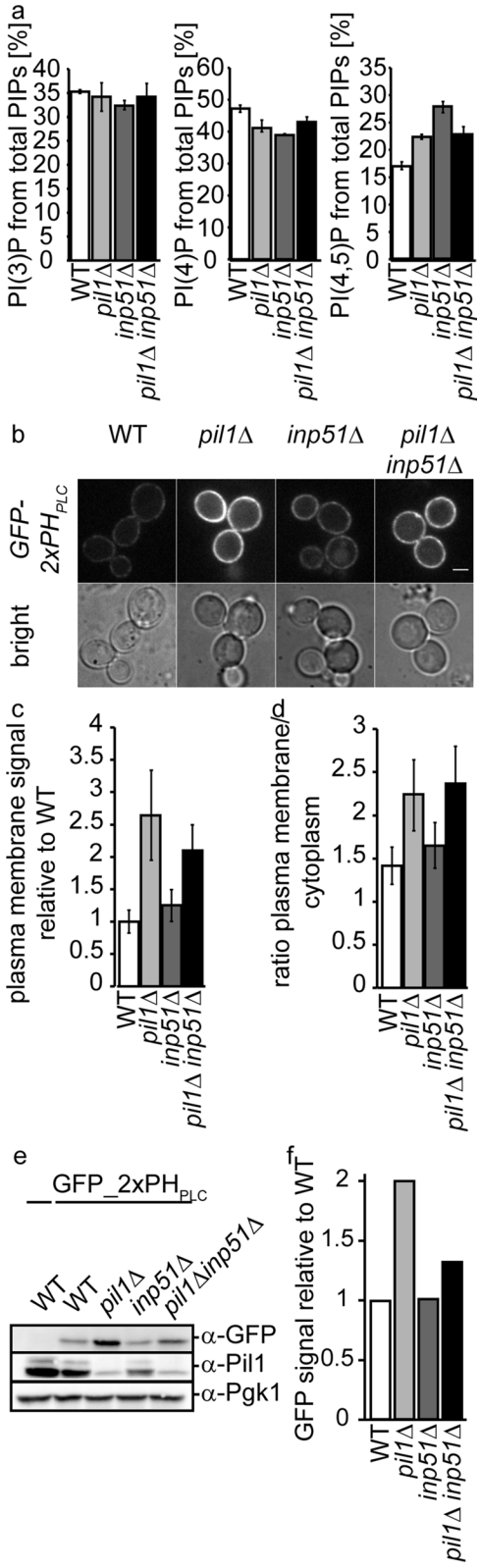

FIGURE 7: *PIL1* is required for normal PI(4,5)P_2 levels at the plasma membrane. (a) Cellular levels of PI(3)P (left), PI(4)P (middle), and PI(4,5)P_2 (right) as percentage of total phosphatidylinositides in WT cells (white bars), *pil1Δ* cells (light gray bars), *inp51Δ* cells (dark gray bars), and *pil1Δinp51Δ* cells (black bars). Error bars represent SDs, $n = 3$. (b) WT (left), *pil1Δ* (middle left), *inp51Δ* (middle right), and *pil1Δinp51Δ* cells (right) expressing two PH domains of phospholipase Cδ under the control of a *CPY* promoter (top). Bottom, corresponding brightfield images. Scale bar, 2.5 μm. (c) Quantification of b. The average intensity of the plasma membrane signal of the GFP-2xPH$_{PLC}^{\delta}$ is plotted. Error bars represent SDs. $n = 39$ (WT), 39 (*pil1Δ*), 36 (*inp51Δ*), and 39 (*pil1Δinp51Δ*). (d) Quantification of b. Ratio of plasma membrane–bound to cytoplasmic signal of the GFP-2xPH$_{PLC\delta}$ domain is plotted. Error bars represent SDs. $n = 39$ (WT), 39 (*pil1Δ*), 36 (*inp51Δ*), and 39 (*pil1Δinp51Δ*). (e) Yeast lysates of WT, *pil1Δ*, *inp51Δ*, and *pil1Δinp51Δ* cells expressing GFP-2xPH$_{PLC\delta}$ and control cells were blotted and probed with antibodies against GFP, Pil1, and Pgk1. (f) Quantification of the GFP signal from e normalized to WT levels.

For SILAC labeling, the lysine prototroph yeast strains W303 WT, W303 *PIL1-GFP*, and W303 *INP51-GFP* were grown according to the protocol for native SILAC (Frohlich *et al.*, 2013) in the presence of normal L-lysine or L-lysine-U-$^{13}C_6$,$^{15}N_2$ (Cambridge Isotope Labs, Tewksbury, MA).

Fluorescence microscopy

Yeast cells from cultures grown to $OD_{600} \approx 0.5$ were mounted with concanavalin A in growth medium, and images were collected on a DeltaVision workstation (Applied Precision, Issaquah, WA) based on an inverted microscope (IX-70; Olympus, Tokyo, Japan) using a 100×/1.4 numerical aperture (NA) oil immersion lens. Images were captured at 24°C with a 12-bit charge-coupled device camera (CoolSnap HQ; Photometrics, Tucson, AZ) and deconvolved using the iterative-constrained algorithm and the measured point spread function.

Alternatively, cells were grown in synthetic medium containing raffinose as carbon source and switched to galactose-containing medium to induce protein expression from a GAL promoter for 2 h. Cells were mounted with concanavalin A and imaged with a spinning-disk confocal microscope (TiLL iMIC CSU22; Andor, Belfast, UK) using a back-illuminated electron-multiplying charge-coupled device camera (iXonEM 897; Andor) and a 100×/1.4 NA oil immersion objective (Olympus). From this setup, 16-bit images were collected using Image iQ (version 1.9; Andor) in the linear range of the camera. For presentation, images were converted to 8-bit images and cropped using ImageJ software (National Institutes of Health, Bethesda, MD).

For quantification of GFP_2xPH$_{PLC\delta}$, images were all acquired with the same settings. The intensity at the plasma membrane and in the cytoplasm was measured using ImageJ. For quantification of the plasma membrane to cytoplasmic signal, the two measured values for each cell were divided.

Affinity purification and mass spectrometry

Inp51-GFP cells or Pil1-GFP cells were grown in the presence of "heavy" lysine (L-lysine-U-$^{13}C_6$,$^{15}N_2$), and WT cells were grown in the presence of normal, "light" lysine. We harvested 500 OD_{600} units of cells by centrifugation and resuspended them in 500 μl of lysis buffer (150 mM KOAc, 20 mM 4-(2-hydroxyethyl)-1-piperazineethanesulfonic acid [HEPES], pH 7.4, 10% glycerol, and complete protease inhibitor cocktail [Roche, Basel, Switzerland]). Zirconia beads (500 μl, 0.1-mm diameter; BioSpec Products, Bartlesville, OK) were added, and cells were lysed using a FASTPREP (MP Biomedicals, Solon, OH) for 60 s at 4°C. Beads were removed by centrifugation, and Triton X-100 was added to a final concentration of 1%. After a 30-min incubation at 4°C, lysates were cleared by centrifugation for 10 min at 1000 × *g*. Equivalent amounts of "light"-labeled control and "heavy"-labeled *PIL1-GFP*–containing lysates or "light"-labeled control and "heavy"-labeled *INP51-GFP*–containing lysates were incubated (separately) with GFP-Trap agarose beads (Allele Biotechnology, San Diego, CA) for 30 min at 4°C. Beads were washed three times with

lysis buffer and three times with wash buffer (150 mM NaCl, 20 mM HEPES, pH 7.4). Beads from *INP51-GFP* pull downs and control pull downs or *PIL1-GFP* and control pull downs were combined in 100 µl of denaturation buffer (8 M urea, 50 mM Tris-HCl, pH 8, 1 mM dithiothreitol) and incubated for 30 min. Proteins were alkylated by the addition of 5.5 mM iodoacetamide for 20 min in the dark and digested with the endoproteinase LysC overnight at 37°C. The resulting peptide mixture was removed from the beads and desalted following the protocol for StageTip purification (Rappsilber *et al.*, 2003). Peptides were subjected to reversed-phase chromatography on a Thermo Easy nLC system connected to a LTQ Orbitrap Velos mass spectrometer (Thermo Fisher Scientific, Waltham, MA) through a nano-electrospray ion source, as described previously (Colombi *et al.*, 2013). The resulting mass spectroscopy (MS) and MS/MS spectra were analyzed using MaxQuant (version 1.4.0.8, www.maxquant.org/; Cox and Mann, 2008; Cox *et al.*, 2011) as described previously (Frohlich *et al.*, 2013). All calculations and plots were performed with the R software package (www.r-project.org/).

Genetic interaction data

Data sets for the analysis of E-MAP data were derived from Surma *et al.* (2013).

Quantification of phosphoinositide levels by high-performance liquid chromatography analysis

Labeling of cells and extraction of phosphoinositides were done as previously described (Audhya and Emr, 2002). Briefly, cells were grown in synthetic medium overnight and kept in log phase. We incubated 5 OD units of cells in inositol-free medium for 15 min and labeled them with 50 µCi of [^{3}H]myo-inositol (MP Biomedicals) for 1 h at room temperature. Cells were then lysed by vortexing samples with glass beads in ice-cold 4.5% perchloric acid for 15 min. Lysates were extracted and spun, and resulting pellets were washed twice with 0.1 mM EDTA. Samples were then deacylated and separated by high-performance liquid chromatography (Shimadzu Scientific Instruments, Kyoto, Japan) and phosphoinositides identified using deacylated ^{32}P standards and an online flow scintillation analyzer (B-RAM; IN/US, Conquer Scientific, San Diego, CA) as described (Devereaux and Di Paolo, 2013).

ACKNOWLEDGMENTS

We thank Christopher G. Burd and Richard J. Chi for critical comments on the manuscript. This work was supported by a Yale Top Scholar Award (to T.C.W.) and National Institutes of Health Grants R01GM095982 (to T.C.W.) and R01DK082700 (to P.D.C.).

REFERENCES

Aguilar PS, Frohlich F, Rehman M, Shales M, Ulitsky I, Olivera-Couto A, Braberg H, Shamir R, Walter P, Mann M, *et al.* (2010). A plasma-membrane E-MAP reveals links of the eisosome with sphingolipid metabolism and endosomal trafficking. Nat Struct Mol Biol 17, 901–908.

Audhya A, Emr SD (2002). Stt4 PI 4-kinase localizes to the plasma membrane and functions in the Pkc1-mediated MAP kinase cascade. Dev Cell 2, 593–605.

Berchtold D, Piccolis M, Chiaruttini N, Riezman I, Riezman H, Roux A, Walther TC, Loewith R (2012). Plasma membrane stress induces relocalization of Slm proteins and activation of TORC2 to promote sphingolipid synthesis. Nat Cell Biol 14, 542–547.

Berchtold D, Walther TC (2009). TORC2 plasma membrane localization is essential for cell viability and restricted to a distinct domain. Mol Biol Cell 20, 1565–1575.

Brach T, Specht T, Kaksonen M (2011). Reassessment of the role of plasma membrane domains in the regulation of vesicular traffic in yeast. J Cell Sci 124, 328–337.

Breslow DK, Cameron DM, Collins SR, Schuldiner M, Stewart-Ornstein J, Newman HW, Braun S, Madhani HD, Krogan NJ, Weissman JS (2008). A comprehensive strategy enabling high-resolution functional analysis of the yeast genome. Nat Methods 5, 711–718.

Collins SR, Schuldiner M, Krogan NJ, Weissman JS (2006). A strategy for extracting and analyzing large-scale quantitative epistatic interaction data. Genome Biol 7, R63.

Colombi P, Webster BM, Frohlich F, Lusk CP (2013). The transmission of nuclear pore complexes to daughter cells requires a cytoplasmic pool of Nsp1. J Cell Biol 203, 215–232.

Cox J, Mann M (2008). MaxQuant enables high peptide identification rates, individualized p.p.b.-range mass accuracies and proteome-wide protein quantification. Nat Biotechnol 26, 1367–1372.

Cox J, Neuhauser N, Michalski A, Scheltema RA, Olsen JV, Mann M (2011). Andromeda: a peptide search engine integrated into the MaxQuant environment. J Proteome Res 10, 1794–1805.

Cremona O, Di Paolo G, Wenk MR, Luthi A, Kim WT, Takei K, Daniell L, Nemoto Y, Shears SB, Flavell RA, *et al.* (1999). Essential role of phosphoinositide metabolism in synaptic vesicle recycling. Cell 99, 179–188.

Devereaux K, Di Paolo G (2013). PI5P migrates out of the PIP shadow. EMBO Rep 14, 214–215.

Di Paolo G, De Camilli P (2006). Phosphoinositides in cell regulation and membrane dynamics. Nature 443, 651–657.

Frohlich F, Christiano R, Walther TC (2013). Native SILAC: metabolic labeling of proteins in prototroph microorganisms based on lysine synthesis regulation. Mol Cell Proteomics 12, 1995–2005.

Frohlich F, Moreira K, Aguilar PS, Hubner NC, Mann M, Walter P, Walther TC (2009). A genome-wide screen for genes affecting eisosomes reveals Nce102 function in sphingolipid signaling. J Cell Biol 185, 1227–1242.

Grossmann G, Malinsky J, Stahlschmidt W, Loibl M, Weig-Meckl I, Frommer WB, Opekarova M, Tanner W (2008). Plasma membrane microdomains regulate turnover of transport proteins in yeast. J Cell Biol 183, 1075–1088.

Grossmann G, Opekarova M, Malinsky J, Weig-Meckl I, Tanner W (2007). Membrane potential governs lateral segregation of plasma membrane proteins and lipids in yeast. EMBO J 26, 1–8.

Hoppins S, Collins SR, Cassidy-Stone A, Hummel E, Devay RM, Lackner LL, Westermann B, Schuldiner M, Weissman JS, Nunnari J (2011). A mitochondrial-focused genetic interaction map reveals a scaffold-like complex required for inner membrane organization in mitochondria. J Cell Biol 195, 323–340.

Janke C, Magiera MM, Rathfelder N, Taxis C, Reber S, Maekawa H, Moreno-Borchart A, Doenges G, Schwob E, Schiebel E, *et al.* (2004). A versatile toolbox for PCR-based tagging of yeast genes: new fluorescent proteins, more markers and promoter substitution cassettes. Yeast 21, 947–962.

Karotki L, Huiskonen JT, Stefan CJ, Ziolkowska NE, Roth R, Surma MA, Krogan NJ, Emr SD, Heuser J, Grunewald K, *et al.* (2011). Eisosome proteins assemble into a membrane scaffold. J Cell Biol 195, 889–902.

Luo G, Gruhler A, Liu Y, Jensen ON, Dickson RC (2008). The sphingolipid long-chain base-Pkh1/2-Ypk1/2 signaling pathway regulates eisosome assembly and turnover. J Biol Chem 283, 10433–10444.

Malinska K, Malinsky J, Opekarova M, Tanner W (2003). Visualization of protein compartmentation within the plasma membrane of living yeast cells. Mol Biol Cell 14, 4427–4436.

Malinska K, Malinsky J, Opekarova M, Tanner W (2004). Distribution of Can1p into stable domains reflects lateral protein segregation within the plasma membrane of living *S. cerevisiae* cells. J Cell Sci 117, 6031–6041.

Mascaraque V, Hernaez ML, Jimenez-Sanchez M, Hansen R, Gil C, Martin H, Cid VJ, Molina M (2013). Phosphoproteomic analysis of protein kinase C signaling in *Saccharomyces cerevisiae* reveals Slt2 mitogen-activated protein kinase (MAPK)-dependent phosphorylation of eisosome core components. Mol Cell Proteomics 12, 557–574.

Milosevic I, Giovedi S, Lou X, Raimondi A, Collesi C, Shen H, Paradise S, O'Toole E, Ferguson S, Cremona O, *et al.* (2011). Recruitment of endophilin to clathrin-coated pit necks is required for efficient vesicle uncoating after fission. Neuron 72, 587–601.

Morales-Johansson H, Jenoe P, Cooke FT, Hall MN (2004). Negative regulation of phosphatidylinositol 4,5-bisphosphate levels by the INP51-associated proteins TAX4 and IRS4. J Biol Chem 279, 39604–39610.

Moreira KE, Schuck S, Schrul B, Frohlich F, Moseley JB, Walther TC, Walter P (2012). Seg1 controls eisosome assembly and shape. J Cell Biol 198, 405–420.

Murphy ER, Boxberger J, Colvin R, Lee SJ, Zahn G, Loor F, Kim K (2011). Pil1, an eisosome organizer, plays an important role in the recruitment

of synaptojanins and amphiphysins to facilitate receptor-mediated endocytosis in yeast. Eur J Cell Biol 90, 825–833.
Olivera-Couto A, Grana M, Harispe L, Aguilar PS (2011). The eisosome core is composed of BAR domain proteins. Mol Biol Cell 22, 2360–2372.
Ong SE, Blagoev B, Kratchmarova I, Kristensen DB, Steen H, Pandey A, Mann M (2002). Stable isotope labeling by amino acids in cell culture, SILAC, as a simple and accurate approach to expression proteomics. Mol Cell Proteomics 1, 376–386.
Pirruccello M, De Camilli P (2012). Inositol 5-phosphatases: insights from the Lowe syndrome protein OCRL. Trends Biochem Sci 37, 134–143.
Rappsilber J, Ishihama Y, Mann M (2003). Stop and go extraction tips for matrix-assisted laser desorption/ionization, nanoelectrospray, and LC/MS sample pretreatment in proteomics. Anal Chem 75, 663–670.
Schuldiner M, Collins SR, Thompson NJ, Denic V, Bhamidipati A, Punna T, Ihmels J, Andrews B, Boone C, Greenblatt JF, *et al*. (2005). Exploration of the function and organization of the yeast early secretory pathway through an epistatic miniarray profile. Cell 123, 507–519.
Schuldiner M, Collins SR, Weissman JS, Krogan NJ (2006). Quantitative genetic analysis in *Saccharomyces cerevisiae* using epistatic miniarray profiles (E-MAPs) and its application to chromatin functions. Methods 40, 344–352.
Singer-Kruger B, Nemoto Y, Daniell L, Ferro-Novick S, De Camilli P (1998). Synaptojanin family members are implicated in endocytic membrane traffic in yeast. J Cell Sci 111, 3347–3356.
Srinivasan S, Seaman M, Nemoto Y, Daniell L, Suchy SF, Emr S, De Camilli P, Nussbaum R (1997). Disruption of three phosphatidylinositol-polyphosphate 5-phosphatase genes from *Saccharomyces cerevisiae* results in pleiotropic abnormalities of vacuole morphology, cell shape, and osmohomeostasis. Eur J Cell Biol 74, 350–360.
Stefan CJ, Audhya A, Emr SD (2002). The yeast synaptojanin-like proteins control the cellular distribution of phosphatidylinositol (4,5)-bisphosphate. Mol Biol Cell 13, 542–557.
Stefan CJ, Padilla SM, Audhya A, Emr SD (2005). The phosphoinositide phosphatase Sjl2 is recruited to cortical actin patches in the control of vesicle formation and fission during endocytosis. Mol Cell Biol 25, 2910–2923.
Stolz LE, Huynh CV, Thorner J, York JD (1998). Identification and characterization of an essential family of inositol polyphosphate 5-phosphatases (INP51, INP52 and INP53 gene products) in the yeast *Saccharomyces cerevisiae*. Genetics 148, 1715–1729.
Stradalova V, Stahlschmidt W, Grossmann G, Blazikova M, Rachel R, Tanner W, Malinsky J (2009). Furrow-like invaginations of the yeast plasma membrane correspond to membrane compartment of Can1. J Cell Sci 122, 2887–2894.
Sun Y, Carroll S, Kaksonen M, Toshima JY, Drubin DG (2007). PtdIns(4,5)P2 turnover is required for multiple stages during clathrin- and actin-dependent endocytic internalization. J Cell Biol 177, 355–367.
Surma MA, Klose C, Peng D, Shales M, Mrejen C, Stefanko A, Braberg H, Gordon DE, Vorkel D, Ejsing CS, *et al*. (2013). A lipid E-MAP identifies Ubx2 as a critical regulator of lipid saturation and lipid bilayer stress. Mol Cell 51, 519–530.
Walther TC, Aguilar PS, Frohlich F, Chu F, Moreira K, Burlingame AL, Walter P (2007). Pkh-kinases control eisosome assembly and organization. EMBO J 26, 4946–4955.
Walther TC, Brickner JH, Aguilar PS, Bernales S, Pantoja C, Walter P (2006). Eisosomes mark static sites of endocytosis. Nature 439, 998–1003.
Walther TC, Mann M (2010). Mass spectrometry-based proteomics in cell biology. J Cell Biol 190, 491–500.
Ziolkowska NE, Christiano R, Walther TC (2012). Organized living: formation mechanisms and functions of plasma membrane domains in yeast. Trends Cell Biol 22, 151–158.
Ziolkowska NE, Karotki L, Rehman M, Huiskonen JT, Walther TC (2011). Eisosome-driven plasma membrane organization is mediated by BAR domains. Nat Struct Mol Biol 18, 854–856.